BCRP Journal of Innovative Research in Science and Technology (BJIRST)

Volume 02, Issue 01, December, 2021, pp. 95-106

CORROSION INHIBITION OF MILD STEEL IN AQUEOUS H_2SO_4 BY THE BIOMOLECULES GUANINE AND GUANOSINE

SukalpaDey[1*], Sanjoy Satpati[2], Aditya Suhasaria[3], Dipankar Sukul[4]

[1]Department of Basic Science and Humanities, Dr. B. C. Roy Polytechnic, Durgapur 713 206, India, Email ID.: sukalpa.dey@bcrec.ac.in

[2]Department of Chemistry, National Institute of Technology, Durgapur 713 209, India, Email ID.: sanjoysatpati91@gmail.com

[3] Department of Chemistry, Government General Degree College, Tehatta, Nadia 741 160, India, Email ID.: suhasaria.aditya@gmail.com

[4]Department of Chemistry, National Institute of Technology, Durgapur 713 209, India. Email ID.: dipankar.sukul@gmail.com

Abstract: ***A pyrine base, guanine and its corresponding nucleoside, guanosine are tested as eco-friendly green corrosion inhibitors for mild steel in 0.5 M aqueous H_2SO_4. Both electrochemical and weight loss techniques are employed for the investigation. Results indicate both the inhibitors exert almost identical inhibition efficiency (around 70% at 3 mM concentration level) with guanosine having slightly greater inhibitory effect. From adsorption isotherm study, types of adsorptions, i.e., physical or chemical has been ascertained. Quantum mechanical study (DFT) allows to indicate the atoms or group of the inhibitor molecules involved in electron donation to the metal or the retro-donation***.

Keywords: ***mild steel; corrosion inhibitor; potentiodynamic polarization; electrochemical impedance; DFT calculation***

1. INTRODUCTION

Corrosion refers to the deterioration of metals. Metals have natural tendency to revert back to its most stabilized oxidized state by the action of oxidizing agents like atmospheric oxygen in the presence of moisture. In acidic aqueous solution, hydronium ion can also play the role of the oxidizing agent. Corrosion of metal not only incurs huge economic losses, but it also damages the natural and historic monuments having immense importance from geographical, archeological and historical viewpoint. As a spontaneous process, corrosion cannot be stopped,

but its rate can be minimized. Various methods to mitigate the menace of corrosion include cathodic protection (by sacrificial metal or impressed current method), application of metallic and non-metallic coating and also the use of organic and inorganic corrosion inhibitors. Corrosion inhibitors can be classified as cathodic or anodic or the mixed type depending on their way of action. Among organic corrosion inhibitors, bio-compatible molecules are preferred over the synthetic organic molecules as the former are less toxic to environment and easily bio-degradable. Different types of bio-relevantenvironmentally benign molecules have been tested and these include various polysaccharides, polymers, amino acids, plant extracts, essential oils,drug molecules, etc [1-10]. These biomolecules impart different extent of corrosion protection (inhibition efficiency varying within the range of 70-95% on an average) depending on the nature of interaction between the biomolecules and metal surface in the particular corrosion environment [1-10]. In this work we report the effect offered by guanine, one of the four main nucleobases present in the nucleic acids DNA and RNA and its nucleoside, guanosine (Fig. 1). Guanine has a fused pyrimidine-imidazole ring system with conjugated double bonds. The molecular arrangement has made guanine planar. In guanosine, guanine is attached to a ribose (ribofuranose) ring via a β-N9-glycosidic bond. Presence of the aromatic ring, π-conjugation, lone pair of electrons present on the heteroatoms, like N and O have made both the molecules ideal candidates for interaction with metal surface and its subsequent corrosion protection. Some initial work indicates these molecules can behave as corrosion inhibitors for steel in aqueous HCl [11]. But detailed anti-corrosion study corroborated with quantum mechanical findings are missing. In this present work, both the electrochemical (potentiodynamic polarization and electrochemical impedance spectroscopy) as well as weight loss method are employed to evaluate their anti-corrosion effectiveness. Adsorption isotherm study is performed. In addition, density functional theory (DFT) calculation provides an insight towards the mode of adsorption of the inhibitor molecules on the metal surface.

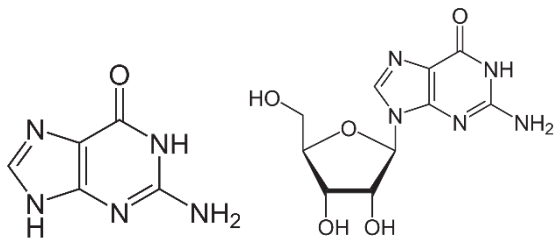

Fig. 1 Structure of guanine (left) and guanosine (right)

2. EXPERIMENTAL SECTION

2.1 Preparation of metal surface for corrosion test

Mild steel coupons are properly treated as reported elsewhere to prepare appropriate surface for electrochemical and weight loss experiment [12-13].

2.2 Electrochemical measurements

Three electrode system with mild steel coupon (exposed area 0.5 cm^2 in 250 mL 0.5 M aqueous H_2SO_4) as the working electrode, saturated calomel electrode (SCE) as the reference and Pt mesh electrode as the auxiliary one is attached with a potentiostat (model: GILL AC, UK). Inhibition efficiency is calculated from potentiodynamic polarization plots from the eq. (1)

$$\eta_{\mathrm{P}}(\%) = \frac{i_{\mathrm{corr}} - i_{\mathrm{corr(inh)}}}{i_{\mathrm{corr}}} \times 100 \qquad (1)$$

where, $i_{\mathrm{corr}}$is the corrosion current density in the uninhibited solution, and $i_{\mathrm{corr(inh)}}$ is in the inhibited one.

Electrochemical impedance experiment is done applying a AC voltage of ± 10 mV with respect to the OCP and with a varied frequency within the range of 100 *k*Hz to 0.01 Hz. The polarization resistance (R_{p}) obtained from the Nyquist plots the inhibition efficiency is calculated as per eq. (2).

$$\eta_{\mathrm{Z}}(\%) = \frac{R_{\mathrm{p}} - R_p^0}{R_{\mathrm{p}}} \times 100 \qquad (2)$$

Here, R_{p} is the polarization resistance as calculated for the inhibited solution and R_{p}^{0} is that for the uninhibited one.

2.3 Weight loss method

From the values of weight loss in the absence and presence of inhibitor (W_0 and W, respectively after 6 h of immersion in 0.5 M H_2SO_4), the inhibition efficiency (η_{W}) is determined following eq. (3).

$$\eta_W(\%) = \frac{W_0 - W}{W_0} \times 100 \quad (3)$$

2.4 Density functional theory (DFT) calculation

DFT study is done usingthe ORCA program (version 2.7.0). B3LYP functional with triple-z quality basis set TZV (P) for N, O and S atoms and double-z quality basis set SV (P) for C and H is employed for geometry optimization ofthe inhibitors. From the energies of the highest occupied molecular orbital (HOMO) and lowest unoccupied molecular orbital (LUMO), various molecular parameters, like the absolute electronegativity (χ, signifies the electron attracting ability of a chemical system), global hardness (η, a parameter signifying the resistance of a chemical system towards charge transfer), and global softness (σ, an indicator of the susceptibility or easiness towards charge transfer)are calculated following the eqs. (4 - 6) [14]

$$\chi = -(E_{HOMO} + E_{LUMO})/2 \quad (4)$$

$$\eta = -(E_{HOMO} - E_{LUMO})/2 \quad (5)$$

$$\sigma = 1/\eta \quad (6)$$

The fraction of total electron density transferred from inhibitor to the metal ($\Delta N_{1\,1\,0}$) is calculated using following eq. (7) :

$$\Delta N_{1\,1\,0} = \frac{(\emptyset_{Fe} - \chi_{inh})}{2(\eta_{Fe} + \eta_{inh})} \quad (7)$$

Here, ϕ_{Fe}, the work function of Fe (1 1 0) surface, is taken as 4.82 eV.The global hardness of Fe (η_{Fe}) is taken as zero, as HOMO and LUMO overlap for the metal [12].

3. RESULT AND DISCUSSION

3.1 Potentiodynamic polarization study

After equilibration, the current response with the variation of applied potential for mild steel in 0.5 M H_2SO_4 in absence and presence of inhibitors are depicted in fig. 2. These plots are known as potentiodynamic polarization plots. The potential when the anodic and cathodic currents become equal is known as corrosion potential (E_{corr}) and the corresponding current is the corrosion current. When divided by the area of exposed surface of the working electrode, it

becomes corrosion current density (i_{corr}) and it's the measure of the corrosion rate. By Tafel extrapolation method, one can determine the values of i_{corr} and E_{corr}. All these values along with the cathodic and anodic Tafel slopes are tabulated in table 1.

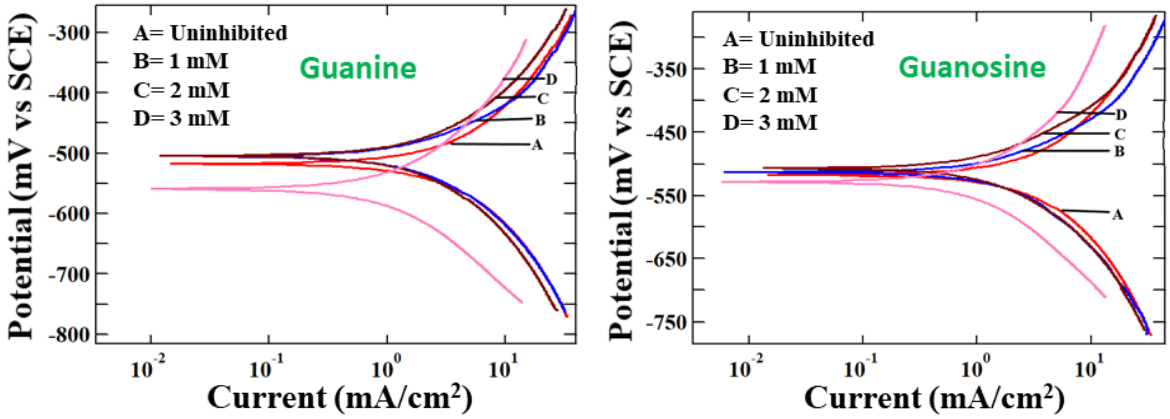

Fig. 2 Potentiodynamic polarization plots of mild steel in 0.5 M H2SO4 on absence and presence of guanine (left) and guanosine (right)

Table 1. Corrosion parameters as derived from the potentiodynamic polarization plots

Inhibitor	Conc. of inhibitor (mM)	$-E_{corr}$ (mV/SCE)	b_a ($mVdec^{-1}$)	$-b_c$ ($mVdec^{-1}$)	i_{corr} ($\mu A\ cm^{-2}$)	η_p%
-	UNINHIBITED	516.4	125.1	143	1987.5	
Guanine	1	505.5	116.7	132.7	1703.4	14.3
	2	505.1	116.4	128.6	1349.2	32.1
	3	556.8	106.5	115.3	647.8	67.4
Guanosine	1	511.82	111.6	124.6	1551.1	22.0
	2	507.3	114.3	124.1	1256.5	36.8
	3	529.6	103.1	111.6	611.7	69.2

Data in Table 1 indicates that with increase in concentration of inhibitors, corrosion current gradually decreases and this results into concomitant increase in the inhibition efficiency. Variation of corrosion potential is not regular. At the lower concentration range, corrosion potential shifts towards more positive direction (noble direction), whereas at the higher concentration it moves towards more negative direction (base direction) with respect to the corrosion potential for uninhibited sample. Cathodic and anodic Tafel slopes also decrease with inhibitor concentration. This suggests reduction of exchange current densities of the cathodic and

anodic reactions at their corresponding equilibrium condition. All such observation is indicative of the mixed type inhibition property of the studied inhibitors, where both the cathodic hydrogen evolution and anodic metal dissolution processes are restricted by the application of inhibitors. If we compare the relative efficiency of the two inhibitors, its seem to be very comparable. Guanosine exerts slightly higher inhibitory action. The ribose ring with free hydroxyl groups seems to the responsible for slightly higher inhibitory propensity. The lone pair of electrons present on the O atoms can interact with the vacant 3d orbitals of Fe atoms. Still data reveals that such interaction is not strong enough and the current density values for both the molecules lie within a range of 10%.

3.2 Electrochemical impedance spectroscopy (EIS)

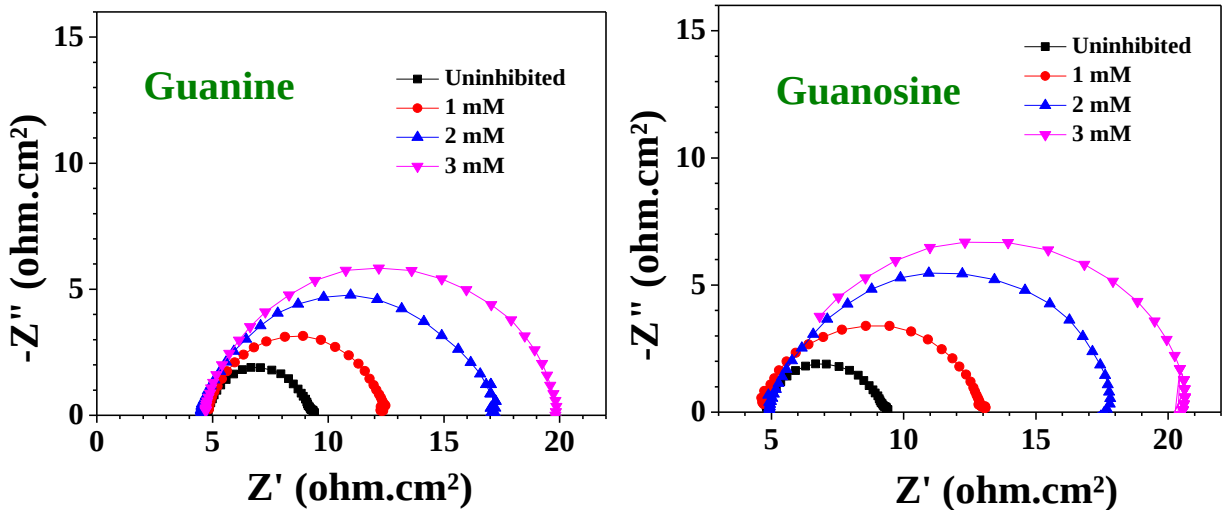

Fig. 3 Nyquist plots of mild steel in in 0.5 M H_2SO_4 in the absence and presence of guanine (left) and guanosine (right)

The Nyquist plots as derived from EIS study in the presence and absence of inhibitors are shown in Fig. 3. The diameter of the capacitive loops increases with inhibitor concentration. This corresponds to enhanced resistance towards charge transfer process at higher inhibitor concentration. In addition, there are other resistive components, like resistance due to adsorbed inhibitor layer and layer of corrosion products formed. All these resistances are clubbed together as polarization resistance (R_p). The capacitive loops are not perfectly semicircle, rather depressed under the real axis. This accounts for the surface heterogeneity. Considering all these experimental observation, the Nyquist plots are fitted by an equivalent circuit as depicted in Fig. 4. This a slightly modified form of a Randles circuit, where the double layer capacitance is

replaced by the CPE (which takes care of the surface heterogeneity). Impedance of CPE comprises of two parameters, Q and n, using which one can calculate the value of C_{dl}. All he fitting parameters are tabulated in Table 2. It shows that the R_p values increase with inhibitor concentration with simultaneous decrease in C_{dl} values. This manifests decrease in effective electroactive area (cathodic and anodic) on the metal surface by adsorption of organic guanine or guanosine layer. The inhibition efficiency calculated from R_p values of uninhibited and inhibited samples are very close, as also observed from potentiodynamic polarization study.

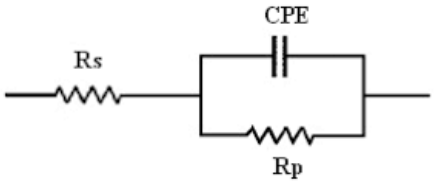

Fig. 4 Equivalent circuit for fitting the Nyquist plots

Table 2 EIS data obtained after fitting the Nyquist plots

Inhibitor	**Conc. (mM)**	**R_P (Ohm cm^2)**	**Q ($\mu\Omega^{-1}$ s^{n}cm^{-2})**	**n**	**C_{dl} (μF cm^{-2})**	**η_z%**	**$\chi 2\times10^4$**
	UNINHIBITED	4.6	993	0.85	413.0	-	4.51
Guanine	1	7.8	789	0.86	344.5	41.0	4.55
	2	12.3	561	0.85	233.1	62.6	4.46
	3	15.6	421	0.86	185.8	70.51	0.46
Guanosine	1	8.4	752	0.86	329.7	45.2	3.26
	2	13.4	465	0.86	203.4	65.7	3.41
	3	16.2	364	0.87	169.0	71.6	3.83

3.3 Weight loss experiment

Not only the electrochemical means, we have performed weight loss method (after 6 h of immersion) also to evaluate the effectiveness of guanine and guanosine for their anti-corrosion property. One advantage of weight loss method is that it provides an overall effect of all possible types of corrosion, uniform, galvanic as well as localized corrosion. At 30 °C and at 3 mM concentration, guanine exerts nearly 65% inhibition efficiency, whereas guanosine offers 67% (Table 3).

Table 3 Corrosion rate and inhibitor efficiency as determined from weight loss experiment

Temp.		Corrosion rate (mg cm^{-2} h^{-1})		η_w (%)	
	Inhibitor conc. (mM)	Guanine	Guanosine	Guanine	Guanosine
30 °C	Uninhibited	5.26914			
	1	3.31429	3.17729	37.1	39.7
	2	2.37638	2.23938	54.9	57.5
	3	1.85474	1.73355	64.8	67.1

3.4 Adsorption isotherm

As corrosion is a surface phenomenon and organic inhibitors are basically adsorption type, one can equalize the inhibition efficiency with the degree of surface covered by the inhibitor layer. Experimental data points are found to fit in complete agreement with the Langmuir adsorption isotherm (eq. 4) [12-13]

$$\frac{C}{\theta} = \frac{1}{K_{ads}} + C \tag{8}$$

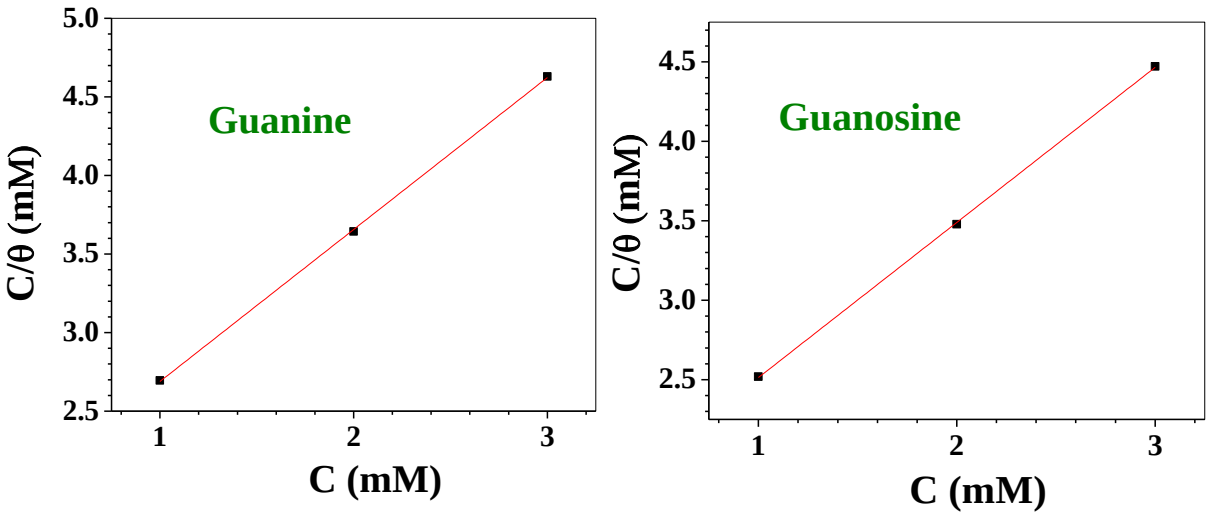

Fig. 5 Langmuir adsorption isotherm plots

Table 4 Adsorption parameters

Inhibitor	TEMP (K)	R^2	Slope	Intercept	$K_{ads}\times10^{-3}$ (molar^{-1})	$-\Delta G^0_{ads}$ (*k*J mol^{-1})
Guanine	303	0.999	0.9671	1.7218	0.58	26.15

Guanosine	303	0.999	0.9760	1.5373	0.65	26.44

where, C is the concentration of inhibitor and K_{ads} is the equilibrium constant of adsorption. Gibbs free energy of adsorption (ΔG^0_{ads}) is related with K_{ads} following the relation (eq. 5):

$$\Delta G^0_{ads} = - RT \ln (55.55 \times K_{ads}) \quad (9)$$

where, 55.55 is the molar concentration of solvent water and it is introduced to make the whole thing within the bracket unitless. From the intercept of C/θ vs. C plot (Fig. 5), we determine the K_{ads} and thereafter ΔG^0_{ads}. Values are shown in table 4. At 30 °C, ΔG^0_{ads} values are found to be about -26 *k*J mol^{-1}. Negative value ascertains the spontaneous nature of adsorption process, whereas the absolute value, which is less than 40 *k*J mol^{-1}, affirms the adsorption process as physisorption [15].

3.5 Result from DFT study

To investigate the mode of adsorption of the inhibitor molecules, i.e. structural moiety of the inhibitor molecule responsible for interaction with the metal surface, we have done the theoretical calculation. We have evaluated the energies of highest occupied molecular orbital (HOMO), lowest unoccupied molecular orbital (LUMO) (Table 5) and the electron distribution at those levels (Fig. 6). From the energy data, other intrinsic molecular parameters are calculated. Interaction of inhibitor molecule and the metal originates from the electron donation from HOMO of the inhibitor to the vacant 3d orbital of Fe, while retro-electron transfer occurs from the filled 4s orbital of Fe to the LUMO of the inhibitor. Higher HOMO and lower LUMO energy facilitate this two-way interaction. Electrochemical and weight loss methods show that both guanine and guanosine provide identical corrosion inhibition efficiency. This suggests similar interaction pattern for both these molecules with mild steel surface in aqueous H_2SO_4. Electron distribution in both the HOMO and LUMO for both the molecules are seen to be distributed over the fused pyrimidine-imidazole ring system together with the carbonyl O attached to the pyrimidine ring. HOMO electron density is also spread over the amine N atom attached to the pyrimidine ring. But the ribose ring of the guanosine is neither involved in HOMO or LUMO electron density distribution pattern. Thus, we can infer that the fused pyrimidine-imidazole ring system along with the carbonyl O connected with the pyrimidine ring) are involved in both the electron donation and acceptance during interaction with the metal. The lone pair of electron

present on N atom in the amine group is associated with the forward electron transfer from inhibitor to metal. The ribose ring of the guanosine is not involved in kind of interaction. This is the reason of nearly equivalent interaction pattern for both the molecules. The energy values of HOMO and LUMO and all the intrinsic molecular parameters are almost of equal values for guanine and guanosine. This confirms that the extent of interaction between the inhibitor molecule and the metal surface is almost the same.Due to all these molecular factors both guanine and guanosine impart comparable corrosion inhibition efficiency.

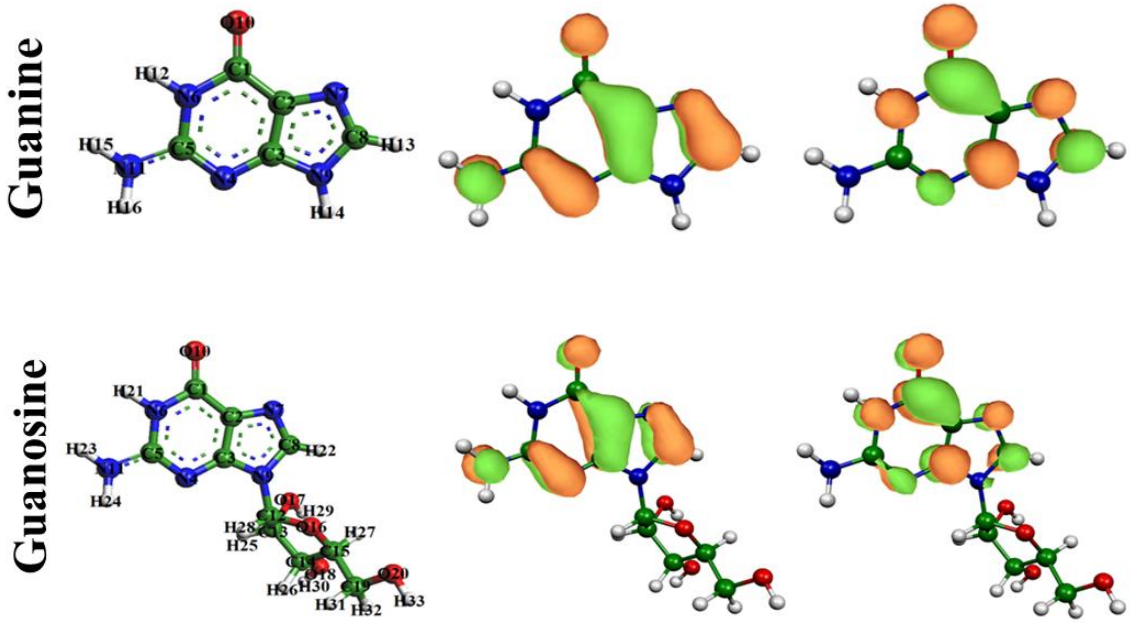

Fig. 6 Energy optimized geometry and electron distribution in HOMO and LUMO

Table 5 Molecular parameters of inhibitors calculated from DFT study.

Inhibitor	E_{HOMO} (eV)	E_{LUMO} (eV)	ΔE (eV)	χ (eV)	η (eV)	σ (eV^{-1})	ΔN
Guanine	-5.9816	-0.6330	5.349	3.31	2.67	0.37	0.28
Guanosine	-5.9876	-0.6384	5.349	3.31	2.67	0.37	0.28

4. CONCLUSION

Guanine and guanosine are shown to provide fair extent of corrosion protection to mild steel in an aggressive corrosive medium of 0.5 M H_2SO_4. Both the inhibitors act as mixed type corrosion inhibitors and their adsorption on mild steel surface in aqueous H_2SO_4 may be categorized as physisorption. DFT result illustrates that the electron distribution in HOMO and LUMO are almost identical for guanosine and guanine. The fused pyrimidine-imidazole moiety along with the carbonyl and amine group attached to the pyrimidine ring are responsible for interaction with metal surface through electron donation and acceptance. The nature and the extent of interaction between the inhibitor and metal surface are almost the same for both the molecules (as revealed by the intrinsic molecular parameters). This accounts for very close corrosion inhibition efficiency offered by the two inhibitors.

ACKNOWLEDGEMENT

SD thanks the Department of Chemistry, NIT Durgapur for allowing to use the experimental infrastructure.

REFERENCES

1. V.S. Sastri, Green corrosion inhibitors: theory and practice, Wiley, 2012.
2. C.Verma, E.E.Ebenso, I.Bahadur, M.A.Quraishi, An overview on plant extracts as environmental sustainable and green corrosion inhibitors for metals and alloys in aggressive corrosive media, J. Mol, Liqs. 266 (2018) 577-590. https://doi.org/10.1016/j.molliq.2018.06.110
3. M. Goyal, S. Kumar, I.Bahadur, C. Verma, E.E.Ebenso, Organic corrosion inhibitors for industrial cleaning of ferrous and non-ferrous metals in acidic solutions: A review, J. Mol, Liqs 256 (2018) 565-573. https://doi.org/10.1016/j.molliq.2018.02.045
4. A. Peter, I. B. Obot, S. K. Sharma, Use of natural gums as green corrosion inhibitors: an overview, Int. J. Indus. Chem 6 (2015) 153–164. https://doi.org/10.1007/s40090-015-0040-1
5. K.Xhanari, M.Finšgar, M.KnezHrnčič, U.Maver, Ž.Knez, B.Seiti, Green corrosion inhibitors for aluminium and its alloys: a review, RSC Adv. 7 (2017) 27299-27330. DOI: 10.1039/C7RA03944A
6. S. M. Z. Hossain, S. A. Razzak, M. M. Hossain, Application of Essential Oils as Green Corrosion Inhibitors, Arab. J. Sci. Engg. 45 (2020) 7137–7159. https://doi.org/10.1007/s13369-019-04305-8
7. M.A. Quraishi, D. SinghChauhan, V. S.Saji, Heterocyclic biomolecules as green corrosion inhibitors, J Mol. Iiqs. 341 (2021) 117265. https://doi.org/10.1016/j.molliq.2021.117265

8. L. Hamadi, S. Mansouri, K. Oulmi, A. Kareche, The use of amino acids as corrosion inhibitors for metals: A review, **Egypt. J. Pet.** 27 (2018) 1157-1165. https://doi.org/10.1016/j.ejpe.2018.04.004
9. B.ElIbrahimi, A. Jmiai, L Bazzi, S.ElIssami, Amino acids and their derivatives as corrosion inhibitors for metals and alloys, Arab. J. Chem. 13 (2020) 740-771. https://doi.org/10.1016/j.arabjc.2017.07.013
10. C. Verma, D.S. Chauhan, M.A. Quraishi, Drugs as environmentally benign corrosion inhibitors for ferrous and nonferrousmaterials in acid environment: An overview, J. Mater. Environ. Sci. 8 (2017) 4040-4051.
11. D.Y. Cruz-Gonzalez, G. Negrón-Silva, D. Angeles-Beltrán, M. Palomar-Pardavé, M. Romero-Romo, H. Herrera-Hernández, Adenine and Guanine Derivative Bases of Purines and Their Corresponding Nucleosides as Corrosion Inhibitors in 1M Hydrochloric Acid, ECS Trans. 36 (2011) 179.
12. S. Satpati, A. Suhasaria, S. Ghosal, A. Saha, S. Dey, D. Sukul, Amino acid and cinnamaldehyde conjugated Schiff bases as proficient corrosion inhibitors for mild steel in 1 M HCl at higher temperature and prolonged exposure: Detailed electrochemical, adsorption and theoretical study, J. Mol. Liq. 324 (2021) 115077. https://doi.org/10.1016/j.molliq.2020.115077
13. P. Roy, S.K.Saha, P. Banerjee, S Dey, D Sukul, Experimental and theoretical investigation towards anti-corrosive property of glutamic acid and poly-γ-glutamic acid for mild steel in 1 M HCl: intramolecular synergism due to copolymerization, Res. Chem.Intermed. 43 (2017) 4423-4444. https://doi.org/10.1007/s11164-017-2887-6
14. P.K. Chattaraj, U. Sarkar, D.R. Roy, Electrophilicity Index, Chem. Rev. 106 (2006) 2065-2091. https://doi.org/10.1021/cr040109f
15. M.A.M. El-Haddad, A.B. Radwan, M.H. Sliem, W.M.I. Hassan, A.M. Abdullah, Highly efficient eco-friendly corrosion inhibitor for mild steel in 5 M HCl at elevated temperatures: experimental & molecular dynamics study, Sci. Rep. 9 (2019) 3695.https://doi.org/10.1038/s41598-019-40149-w